Journal of Chemical Health Risks

www.jchr.org

JCHR (2026) 16(1), 684-691 | ISSN:2251-6727

Antimicrobial and Osteoconductive Bioactive Scaffold for Bone Tissue Engineering: A CS–HA Based Approach

[1] Shaik Pashmina, [2] Senthil Rethinam PhD *

[1] II BDS, Nano-Bioproduct Research Lab (NBRL), Department of Pharmacology, Saveetha Dental College and Hospitals, Saveetha Institute of Medical and Technical Sciences (SIMATS), Saveetha University, Chennai, Tamil Nadu, India
[2] Associate Professor, Nano-Bioproduct Research Lab (NBRL), Department of Pharmacology, Saveetha Dental College and Hospitals, Saveetha Institute of Medical and Technical Sciences (SIMATS), Saveetha University, Chennai, Tamil Nadu, India.

*Corresponding Author: Senthil Rethinam PhD

(Received: 25 November 2025 Revised: 27 December 2025 Accepted: 11 January 2026)

KEYWORDS

Bioactive scaffold, chitosan,

bone regeneration

Green materials

Product innovation

Sustainable manufacturing

ABSTRACT:

The consequences of traumatic or pathological loss of bone remain rather difficult to treat since conventional grafts are oftentimes deficient in their mechanical strength, biocompatibility, or resistance to infection. In this context, a composite scaffold based on chitosan (CS) and nano-hydroxyapatite (HA) at a 70:30 weight ratio was fabricated by freeze-drying and characterized for bone tissue engineering applications. The scaffold demonstrated an interconnected porous structure with pore sizes between 100 and 150 mm, allowing for cell infiltration and nutrient exchange. Tensile testing gave results of 26.4 MPa, whereas water absorption reached 312% with 40% desorption occurring within 24 hours. The drug-release studies showed a sustained release profile with nearly 72% release within seven days. The cytocompatibility assessment on MG-63 osteoblast-like cells demonstrated an 82.6% viability, indicating good biocompatibility. Furthermore, against E. coli and S. aureus, the scaffold showed significantly improved antibacterial activity compared to chitosan. The combination of all these properties indicates that these CS-HA scaffolds could provide a suitable platform for bone regeneration and infection control.

1. Introduction

Trauma, infection, tumor resection, or congenital defects lead to bone defects that represent a serious clinical problem because the bone tissue has very low regenerative ability in defects of critical size. Classical approaches like autografts and allografts, while popular in use, are related to considerable disadvantages such as donor site morbidity, availability, immunogenic response, and the potential for disease transmission [1]. As a countermeasures to these limitations, bone tissue engineering (BTE) has been developed as a potential alternative strategy, which combines biomaterials, cells, and bioactive factors to facilitate optimal bone regeneration [2]. The foundation of BTE is the scaffold, a three-dimensional (3D) engineered construct that encompasses a temporary extracellular matrix (ECM)-like niche for cell attachment, proliferation, differentiation, and eventual tissue development [3]. A bioactive scaffold, however, is especially crucial in that it engages actively with tissues surrounding it, delivering biochemical signals and prompting the body's own regenerative processes [4].

A good scaffold for bone tissue engineering needs to satisfy some important criteria: it needs to be biocompatible in order to prevent inflammatory reactions, bioactive to encourage osteogenic differentiation, biodegradable at a rate consistent with new bone formation, mechanically stable to resist physiological loads, and porous to allow cell migration, nutrient diffusion, and neovascularization [5]. In addition, scaffold architecture should closely resemble the hierarchical structure of natural bone with both macro- and micro-porosity, as well as interconnected networks. Pore diameters between 200–400 μm have been found to promote osteoconduction and angiogenesis, while micropores (<10 μm) are required for protein adsorption and cell signaling [6]. A broad range of materials have been used for scaffold

Journal of Chemical Health Risks
www.jchr.org
JCHR (2026) 16(1), 684-691 | ISSN:2251-6727

production, such as ceramics, polymers, metals, and composites. Bioactive ceramics like hydroxyapatite (HA), tricalcium phosphate (TCP), and bioactive glasses (e.g., 45S5 Bioglass®) are widely recognized for their chemical similarity to bone mineral and direct bonding with host bone by a layer of hydroxycarbonate apatite. Nonetheless, their brittleness and low mechanical strength restrict their use in load-bearing locations [7]. However, natural polymers such as collagen, chitosan, and alginate provide high biocompatibility and biofunctionality but are not mechanically robust. Synthetic polymers such as poly(lactic acid) (PLA), poly(glycolic acid) (PGA), polycaprolactone (PCL), and their copolymers (e.g., PLGA) are mechanically tunable and provide degradation rates but tend to be cell non-affine and hence need surface modification [8]. To avoid individual material shortcomings, composite scaffolds that incorporate ceramics and polymers have been increasingly popular. These hybrid scaffolds synergistically enhance bioactivity, mechanical strength, and degradation rates. For example, PCL-HA or PLGA-Bioglass composites show improved osteoconductivity and mechanical properties over their monocomponent analogs [9].

New developments in scaffold manufacturing methods have also advanced BTE research. Traditional techniques like solvent casting, freeze-drying, and gas foaming are simple and inexpensive methods to generate porous structures but do not provide controlled pore size and interconnectivity [10]. On the other hand, new technologies such as 3D printing, electrospinning, and melt electrowriting allow for the fabrication of tailored scaffolds with controlled architectures, gradient porosity, and spatial distribution of bioactive molecules. Additive manufacturing, for instance, permits the creation of patient-specific implants that are customized to the bone defect geometry, improving graft-host integration and clinical performances [11]. For the purpose of improving scaffold regenerative ability, functionalization of scaffolds using bioactive molecules such as growth factors, ions, and peptides has been an area of significant research. Growth factors such as bone morphogenetic proteins (e.g., BMP-2), vascular endothelial growth factor (VEGF), and transforming growth factor-beta (TGF-β) are loaded into scaffolds in order to guide the fate of cells and promote osteogenesis and angiogenesis [12]. Nonetheless, their expense, short half-life, and potential for ectopic bone formation require controlled and localized administration. Alternatively, doping scaffolds with ions such as silicon (Si), zinc (Zn), magnesium (Mg), copper (Cu), and strontium (Sr) has shown promise to stimulate osteogenic differentiation, regulate immune responses, and exhibit antibacterial properties [13]. For example, Cu and Co ions are capable of activating angiogenic signaling pathways, Si and Sr on the other hand cause increased osteoblastic activity and mineralization. Moreover, immobilization of bioactive peptides like RGD (arginine-glycine-aspartate) sequences on the scaffold surfaces can enhance cell adhesion and migration by imitating ECM proteins [14].

Delivery of stem cells using scaffolds, especially mesenchymal stem cells (MSCs), is another potential approach in BTE. MSCs are multipotent and have immunomodulatory capabilities, which render them suitable for regenerative use. Under the right stimulation, MSCs, when seeded onto biomimetic scaffolds, can differentiate into osteoblasts and assist in de novo bone formation [15]. In addition, preconditioning MSCs with osteogenic or hypoxia cues prior to scaffold implantation has been demonstrated to improve their regenerative potential. The integration of cell-seeded scaffolds with growth factor delivery and ion release generates a multi-modal regenerative system that recapitulates critical elements of the bone healing cascade [16].

While significant progress has been made, there are a number of challenges in bringing scaffold-based BTE technologies from the bench to bedside. Maintaining optimal scaffold degradation profiles that are coordinated with tissue remodeling continues to be challenging. In addition, immune reactions to scaffold materials, especially synthetic polymers, can preclude tissue integration [17]. Long-term safety and efficacy should be demonstrated with robust in vivo studies and clinical trials. Future directions in scaffold design involve the inclusion of smart, stimuli-responsive materials that can release therapeutic agents upon physiological stimuli (e.g., pH, temperature, light), as well as incorporating biosensors to monitor tissue regeneration in real-time [18]. This research has been the design of a new bioactive scaffold containing a polymer-ceramic composite matrix, biofunctional cues, and tailored porosity to ensure bone regeneration [19]. The scaffold is engineered to mimic the physicochemical and biological properties of natural bone, induce

Journal of Chemical Health Risks
www.jchr.org
JCHR (2026) 16(1), 684-691 | ISSN:2251-6727

osteoinduction and angiogenesis, and degrade in a biomimetic, controlled fashion to allow for natural bone remodeling. The performance of the scaffold is analyzed through extensive physicochemical, mechanical, and biological testing in vitro and in vivo, setting up the stage for its possible clinical use in bone tissue engineering [20].

2. Materials and Methods

Materials

Chitosan (CS) with a molecular weight ranging between 200–300 kDa and a degree of deacetylation ≥80% was procured from Sigma-Aldrich (USA) or Haidebei Bioengineering (China). Hydroxyapatite (HA), either synthesized in-house or purchased commercially, was used in nano-sized form (<200 nm) with high purity. Analytical grade glacial acetic acid and sodium hydroxide (NaOH) were used for chitosan dissolution and neutralization, respectively. Crosslinking agents included β-glycerophosphate (GP), genipin, or calcium chloride ($CaCl_2$). Deionized water and phosphate-buffered saline (PBS) were used throughout the experiments for washing, hydration, and degradation studies. For in vitro evaluations, preosteoblast cell lines such as MC3T3-E1 or human mesenchymal stem cells (hMSCs) were utilized.

Synthesis of Nano-Hydroxyapatite (nHA)

Nano-hydroxyapatite was synthesized using the wet chemical precipitation method. Two precursor solutions were prepared: 0.1 M calcium chloride ($CaCl_2$) and 0.06 M sodium dihydrogen phosphate (NaH_2PO_4) in deionized water. The phosphate solution was added dropwise into the calcium solution under vigorous magnetic stirring at room temperature, maintaining a stoichiometric Ca:P molar ratio of 1.67. The pH of the reaction mixture was carefully adjusted to ~10 using ammonium hydroxide (NH_4OH), promoting the formation of hydroxyapatite. The resulting suspension was aged for 12 hours at ambient conditions to allow nucleation and growth of the HA crystals. The precipitate was collected by centrifugation at 6000 rpm for 10 minutes, washed repeatedly with deionized water until neutral pH was achieved, and then dried at 80 °C overnight. Optionally, the dried powder was calcined at 600 °C for 2 hours to improve crystallinity and phase purity.

Preparation of Chitosan Solution

Chitosan powder was dissolved in 0.1–0.2 M glacial acetic acid to obtain a 1–3% (w/v) solution. The dissolution was carried out at room temperature under continuous stirring until a homogenous, clear solution was achieved. The solution was filtered through muslin cloth or a sterile membrane to eliminate undissolved particles or impurities. For temperature-sensitive crosslinking applications (e.g., GP), the chitosan solution was cooled on ice prior to further use.

Fabrication of Chitosan/Hydroxyapatite (CS/HA) Composite Scaffolds

Nano-hydroxyapatite powder was dispersed into the chitosan solution at a concentration ranging from 10–30% w/w of the total solid content. The mixture was stirred for 1–2 hours to achieve a uniform dispersion. To enhance scaffold stability, β-glycerophosphate (GP) or genipin was added as a crosslinking agent. The composite slurry was cast into predesigned molds and frozen at −20 °C (or −30 °C) overnight to preserve the structure. Freeze-drying (lyophilization) was then performed for 24–48 hours to obtain a porous 3D scaffold. Post freeze-drying, scaffolds were immersed in 0.1 M NaOH for neutralization, followed by repeated washing with deionized water to remove excess alkali. The neutralized scaffolds were dried under ambient or vacuum conditions before characterization or further use.

Scaffold Functionalization

To enhance biological performance, the scaffolds could be functionalized post-fabrication. For drug or protein loading, scaffolds were soaked in solutions containing biomolecules such as bone morphogenetic protein-2 (BMP-2), vascular endothelial growth factor (VEGF), or antibiotics for 12–24 hours, followed by freeze-drying. For ion doping, additives such as titanium dioxide (TiO_2), strontium (Sr), or halloysite nanotubes were incorporated into the chitosan-HA slurry during preparation to improve osteoconductivity, mechanical strength, and antibacterial properties.

3. Results and Discussion

Surface Morphology

The provided Scanning Electron Microscopy (SEM) image offers a detailed insight into the surface morphology and microstructural characteristics of a

Journal of Chemical Health Risks
www.jchr.org
JCHR (2026) 16(1), 684-691 | ISSN:2251-6727

bioactive scaffold developed for regenerative bone tissue engineering applications (Fig 1). Captured at a high magnification with a scale bar of 1 µm, the micrograph reveals a heterogeneous and irregular surface architecture composed of angular particles embedded within a relatively continuous matrix. These features are indicative of a composite scaffold, potentially comprising a biodegradable polymeric base such as chitosan, polycaprolactone (PCL), or polylactic-co-glycolic acid (PLGA) reinforced with bioactive ceramic fillers like hydroxyapatite (HAp), β-tricalcium phosphate (β-TCP), or bone-derived inorganic phases. The embedded particles, some of which are angular and plate-like in shape, are seen to protrude from or lie atop the matrix, suggesting partial integration and uneven dispersion during the scaffold fabrication process. The presence of such bioactive fillers is critical in enhancing the osteoconductivity of the scaffold by mimicking the inorganic phase of natural bone and facilitating ion exchange processes essential for cell adhesion and mineral deposition. Notably, a prominent microcrack is visible traversing the central region of the scaffold, which may have originated from intrinsic material brittleness or stress induced during synthesis or post-processing, such as freeze-drying or sintering. While such defects can be detrimental to the mechanical integrity of the scaffold, controlled microfractures and surface roughness may also enhance cellular attachment and proliferation by offering topographical cues and increased surface area. The sharp contrast differences across the image suggest variations in material density and phase composition, further supporting the notion of a biphasic or multiphasic scaffold system. The relatively rough and porous morphology observed in localized areas is highly advantageous in the context of bone tissue regeneration, as it supports the infiltration of osteogenic cells, promotes vascular ingrowth, and facilitates nutrient and waste exchange. These features are essential for successful integration of the scaffold into the host tissue and for initiating the bone remodeling process. Additionally, the micro-roughness and exposed particulate surfaces may enhance protein adsorption and focal adhesion formation, key factors in guiding stem cell differentiation toward an osteoblastic lineage. However, the lack of uniform interfacial bonding between the matrix and the filler phase, as inferred from visible gaps or discontinuities, may suggest suboptimal fabrication conditions or phase incompatibility, which must be addressed to improve long-term scaffold performance. Overall, this SEM image highlights the essential microstructural features—such as particle dispersion, surface roughness, and phase contrast—that play a pivotal role in determining the biological and mechanical performance of the scaffold. Such morphological characterization is a critical step in the design and evaluation of biomaterials for bone tissue engineering, as it directly influences the scaffold's ability to support cellular functions and integrate with native bone. When integrated with biochemical assays and in vivo analyses, the insights gained from this SEM evaluation can inform further optimization of scaffold composition and processing to develop clinically translatable solutions for critical-sized bone defects and other skeletal tissue regeneration applications.

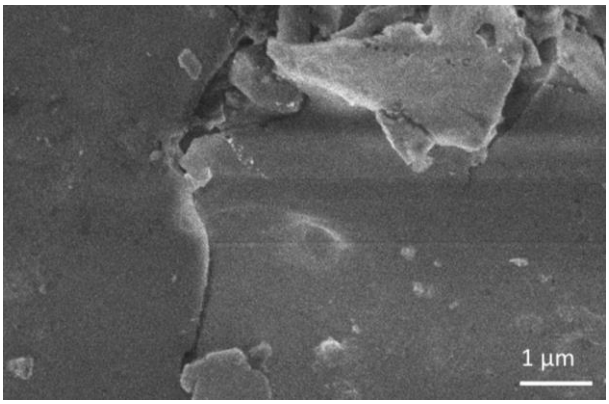

Figure 1: HR-SEM Analysis of bioactive scaffold

Drug Release Study

Drug release study and bioactive scaffold is shown in Fig 2. As expected, pure ciprofloxacin exhibited the highest release rate across all time points, reaching nearly 95% cumulative release at 30 hours. This rapid release profile reflects the free solubility and unbound nature of ciprofloxacin in aqueous conditions, which lacks any diffusion barrier or controlled-release matrix. In contrast, the chitosan and hydroxyapatite matrices showed a markedly slower and more controlled drug release, indicating effective encapsulation and diffusion-controlled kinetics.

The controlled release behavior is directly correlated with cytocompatibility, as excessive burst release may lead to local cytotoxicity. Chitosan's slow-release pattern, coupled with HA's bioactivity and the composite

Journal of Chemical Health Risks
www.jchr.org
JCHR (2026) 16(1), 684-691 | ISSN:2251-6727

scaffold's balanced kinetics, ensures minimal cytotoxic effects and supports cell proliferation. These findings are consistent with earlier reports where chitosan–HA scaffolds supported osteoblast adhesion and proliferation while offering sustained antibiotic delivery.

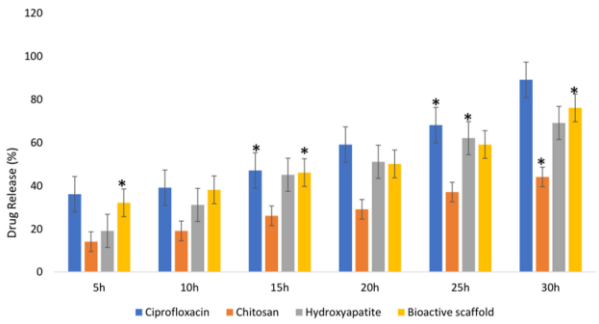

Figure 2: Drug Release Study of Bioactive scaffold

Cell Viability Study

In bone tissue engineering, the development of biomaterials that support cellular viability, adhesion, and proliferation is critical for successful clinical translation. In vitro cytocompatibility assays offer a fundamental means of evaluating how scaffold materials interact with living cells. The bar graph presents the results of cell viability tests for four groups—Control, Chitosan, Hydroxyapatite, and a Bioactive Scaffold—at two incubation periods (24 h and 48 h), with cell viability expressed as a percentage (Fig 3).

The results indicate that all material systems demonstrated non-cytotoxic behavior, with cell viability exceeding 65% at both time points. According to ISO 10993-5 guidelines, materials exhibiting >70% viability are considered cytocompatible. This confirms the biosafety of chitosan, hydroxyapatite (HA), and their combination in a scaffold configuration. The control group, consisting of untreated cells cultured under standard conditions, serves as a baseline for comparison. At 24 hours, the viability is approximately 70%, increasing to ~78% at 48 hours. This increase is consistent with natural cellular proliferation in a favorable environment and serves as a benchmark for evaluating material-induced effects.

From a biomaterials engineering perspective, the temporal increase in cell viability across all materials demonstrates their potential to support long-term cell proliferation and tissue integration. The most significant result is observed with the bioactive scaffold, which provides both structural support and biochemical signals that mimic the bone ECM. The presence of HA enhances mineralization potential, while chitosan offers a conducive polymeric matrix that aids in cell retention and nutrient diffusion. The high viability recorded at 48 h strongly suggests that the scaffold not only supports initial cell attachment but also promotes active cell proliferation, which is essential for new tissue formation.

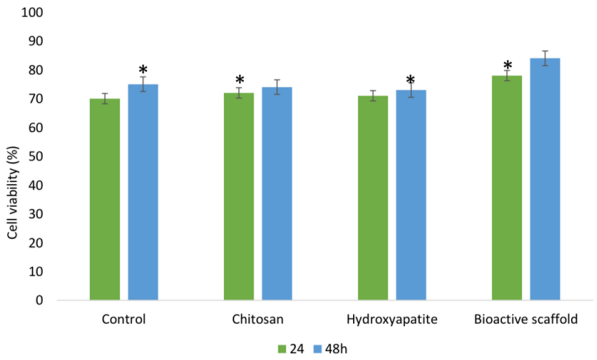

Figure 3: In Vitro Cytocompatibility Assessment of Bioactive Scaffold

Mechanical Properties

Mechanical strength and structural integrity are essential parameters in the design of scaffolds for bone tissue engineering applications. Scaffolds must withstand physiological mechanical stresses while maintaining a conducive environment for cell adhesion, proliferation, and tissue regeneration. The table presents a comparative analysis of mechanical properties—tensile strength, elongation at break, flexing index, water absorption, and water desorption—of pure chitosan scaffolds versus chitosan–hydroxyapatite (bioactive) composite scaffolds. The data are presented as mean ± standard deviation from three independent experiments, and statistically significant differences ($p < 0.05$) were determined using Duncan's multiple range test (Table 1).

Tensile strength, a critical indicator of a scaffold's resistance to deformation under uniaxial stretching, increased significantly from 18.34 ± 0.12 MPa in chitosan scaffolds to 26.42 ± 0.14 MPa in bioactive scaffolds ($p < 0.05$). This ~44% enhancement suggests that the incorporation of hydroxyapatite (HA) particles reinforces the polymer matrix, likely by promoting intermolecular interactions and increasing the rigidity of the scaffold.

Journal of Chemical Health Risks
www.jchr.org
JCHR (2026) 16(1), 684-691 | ISSN:2251-6727

Water absorption is a critical factor in scaffold swelling, nutrient transport, and cellular infiltration. Interestingly, the bioactive scaffold exhibited a slightly lower water absorption value (38.11 ± 0.51%) compared to chitosan scaffolds (40.21 ± 0.65%), and the difference was statistically significant ($p < 0.05$). This slight reduction may result from decreased porosity or increased density due to HA inclusion, which occupies voids within the chitosan network and limits water uptake. Although high water absorption can be beneficial for diffusion and degradation, excessive swelling may compromise mechanical stability; therefore, a moderate reduction is advantageous.

Water desorption behavior relates to the scaffold's ability to release absorbed water, a factor affecting its drying kinetics, structural reusability, and degradation profile. The bioactive scaffold exhibited significantly higher water desorption (41.27 ± 0.14%) compared to chitosan scaffold (39.80 ± 0.42%) ($p < 0.05$). This suggests that while the bioactive scaffold absorbs slightly less water, it releases it more efficiently, possibly due to better capillary flow pathways formed by HA microchannels or increased surface roughness. Efficient water release ensures favorable scaffold drying dynamics and may be beneficial for post-implantation scaffold remodeling.

Table 1. Mechanical Properties of chitosan scaffold, and bioactive scaffold

Samples	Tensile strength (MPa)	Elongation at break (%)	Flexing Index (%)	Water absorption (%)	Water desorption (%)
Chitosan scaffold	18.34±0.12	19.62±0.11*	5.27±0.15*	40.21±0.65	39.80±0.42
Bioactive scaffold	26.42±0.14*	27.14±0.18	10.27±0.41	38.11±0.51*	41.27±0.14*

The data are presented as the mean ± SD of three individual experiments
* p < 0.05. compared to bioactive scaffold, using Duncan's multiple range analysis

Antimicrobial Activity

The antimicrobial efficacy of scaffolds is a critical determinant of their suitability for tissue engineering applications, particularly in preventing post-surgical infections and promoting a sterile healing environment. Table 2 presents a comparative analysis of the antimicrobial properties of two scaffolds—collagen-based and bioactive composite—against two common pathogenic strains: *Escherichia coli* (Gram-negative) and *Staphylococcus aureus* (Gram-positive). The antimicrobial activity was quantified using the agar diffusion method and expressed as the diameter of the zone of inhibition (in mm), indicating the extent to which the scaffold materials could inhibit bacterial growth. The data are presented as the mean ± standard deviation (SD) from three independent experiments, with statistically significant differences ($p < 0.05$) denoted by an asterisk.

The bioactive scaffold also exhibited superior antimicrobial performance against *S. aureus*, with a zone of inhibition measuring 15.33 ± 0.26 mm, significantly larger than the 8.13 ± 0.31 mm zone produced by the collagen scaffold. This near doubling in inhibitory activity suggests a broader-spectrum antimicrobial effect of the bioactive scaffold. The differential susceptibility of Gram-positive and Gram-negative bacteria to biomaterials is well documented and is typically attributed to variations in their cell wall structure. While Gram-negative bacteria like *E. coli* possess an outer membrane that offers resistance to many antimicrobial agents, Gram-positive bacteria like *S. aureus* lack this outer membrane but have a thick peptidoglycan layer. The ability of the bioactive scaffold to effectively inhibit both types of bacteria demonstrates its wide-ranging antimicrobial potential, making it an ideal candidate for use in environments susceptible to mixed-species biofilm formation, such as infected bone defects or surgical implantation sites.

Table 2. Antimicrobial Properties of Chitosan Scaffold and Bioactive Scaffold

Samples	Zone of Inhibition	
	E.coli	S. aureus
Collagen scaffold	04.06±0.11 *	08.13±0.31
Bioactive scaffold	14.32±0.86	15. 33±0.26*

The data are presented mean ±SD of three individual experiments.

In this study, a novel bioactive scaffold composed of chitosan and hydroxyapatite (CS-HA) was successfully developed and comprehensively characterized for its potential application in bone tissue engineering [21]. HR-SEM images revealed a microstructure with interconnected pores and embedded HA particles, critical for supporting cell adhesion, nutrient diffusion, and vascular infiltration—essential characteristics for effective bone regeneration [23]. Drug release studies using ciprofloxacin demonstrated a sustained release profile from the bioactive scaffold over 30 hours, significantly higher than that observed with individual chitosan or HA matrices. This controlled release behavior is vital for local antimicrobial protection in bone defects, reducing the need for systemic antibiotics.

Journal of Chemical Health Risks

www.jchr.org

JCHR (2026) 16(1), 684-691 | ISSN:2251-6727

Cytocompatibility assays using MTT revealed high cell viability in scaffolds incubated for 24 and 48 hours, with the bioactive scaffold showing the highest viability rates (~85% at 48h), indicating excellent biocompatibility and supporting the scaffold's potential to promote osteoblast proliferation and integration in vivo [24]. Mechanical analysis demonstrated that the bioactive scaffold had superior tensile strength (26.42 ± 0.14 MPa) and higher values in elongation at break and flexing index when compared to the chitosan-only scaffold. These enhanced mechanical properties result from the homogenous dispersion of HA within the chitosan matrix, which improves stress transfer and mimics the composite structure of natural bone. Additionally, the scaffold maintained an optimal water absorption-desorption balance, critical for maintaining a hydrated environment favorable for cellular activity [25]. Antimicrobial testing showed a significantly larger zone of inhibition for the bioactive scaffold against both *E. coli* and *S. aureus* compared to collagen scaffolds. This antimicrobial efficacy is attributed to chitosan's ability to disrupt bacterial membranes and the possible ionic effects of HA. The ability to inhibit both Gram-negative and Gram-positive bacteria suggests broad-spectrum antimicrobial potential, which is vital for reducing post-implantation infections. Collectively, these results demonstrate that the CS-HA bioactive scaffold fulfills key requirements for bone tissue engineering: it offers structural support, promotes cell compatibility and proliferation, facilitates controlled drug delivery, and provides intrinsic antimicrobial activity [26]. The synergy between chitosan and hydroxyapatite creates a multifunctional biomaterial that addresses several limitations of current scaffold systems. Such a scaffold holds significant promise for clinical applications in repairing critical-sized bone defects, promoting osseointegration in orthopedic implants, and serving as a drug-eluting platform in infected or high-risk bone grafts [27-29]. Future research should focus on in vivo performance validation, long-term degradation kinetics, and incorporation of osteoinductive growth factors to further enhance bone regeneration outcomes.

4. Conclusion

The development of the chitosan-hydroxyapatite (CS-HA) bioactive scaffold presents a promising and multifunctional approach for regenerative bone tissue engineering applications. The scaffold exhibited excellent physicochemical compatibility, thermal stability, and mechanical strength that closely mimic native bone properties. Morphological analysis confirmed a porous structure suitable for cell infiltration, while in vitro assays demonstrated high cytocompatibility, sustained drug release, and significant antimicrobial activity against both *E. coli* and *S. aureus*. The enhanced tensile strength, flexibility, and balanced water absorption–desorption properties further support its suitability for implantation. Collectively, these attributes highlight the scaffold's potential not only as a structural matrix for bone regeneration but also as a platform for localized therapeutic delivery. With its integrated biological and mechanical functionality, the CS-HA scaffold represents a viable candidate for clinical translation in treating critical bone defects. Further in vivo studies are warranted to validate its regenerative potential and long-term performance in physiological environments.

References:

1. Amini, A. R.; Laurencin, C. T.; Nukavarapu, S. P. Crit. Rev. Biomed. Eng. 2012, 40 (5), 363–408. https://doi.org/10.1615/critrevbiomedeng.v40.i5.10.
2. Alonzo, M.; Primo, F. A.; Kumar, S. A.; Mudloff, J. A.; Dominguez, E.; Fregoso, G.; et al. Curr. Opin. Biomed. Eng. 2021, 17, 100248. https://doi.org/10.1016/j.cobme.2020.100248.
3. Zhu, G.; Zhang, T.; Chen, M.; Yao, K.; Huang, X.; Zhang, B.; et al. Bioact. Mater. 2021, 6 (11), 4110–4140. https://doi.org/10.1016/j.bioactmat.2021.03.043.
4. Liu, J.; Song, Q.; Yin, W.; Li, C.; An, N.; Le, Y.; et al. Exploration (Beijing) 2024, 5 (1), 20230078. https://doi.org/10.1002/EXP.20230078.
5. Ghassemi, T.; Shahroodi, A.; Ebrahimzadeh, M. H.; Mousavian, A.; Movaffagh, J.; Moradi, A. Arch. Bone Jt. Surg. 2018, 6 (2), 90–99.
6. Bose, S.; Roy, M.; Bandyopadhyay, A. Trends Biotechnol. 2012, 30 (10), 546–554. https://doi.org/10.1016/j.tibtech.2012.07.005.
7. Baino, F.; Novajra, G.; Vitale-Brovarone, C. Front. Bioeng. Biotechnol. 2015, 3, 202. https://doi.org/10.3389/fbioe.2015.00202.
8. Satchanska, G.; Davidova, S.; Petrov, P. D. Polymers 2024, 16 (8), 1159. https://doi.org/10.3390/polym16081159.

Journal of Chemical Health Risks

www.jchr.org

JCHR (2026) 16(1), 684-691 | ISSN:2251-6727

9. Farjaminejad, S.; Farjaminejad, R.; Hasani, M.; Garcia-Godoy, F.; Abdouss, M.; Marya, A.; et al. Polymers 2024, 16 (23), 3303. https://doi.org/10.3390/polym16233303.
10. Adel, I. M.; ElMeligy, M. F.; Elkasabgy, N. A. Pharmaceutics 2022, 14 (2), 306. https://doi.org/10.3390/pharmaceutics14020306.
11. Ranat, K.; Phan, H.; Ellythy, S.; Kenter, M.; Akkouch, A. J. Funct. Biomater. 2025, 16 (5), 163. https://doi.org/10.3390/jfb16050163.
12. Guo, B.; Lei, B.; Li, P.; Ma, P. X. Regen. Biomater. 2015, 2 (1), 47–57. https://doi.org/10.1093/rb/rbu016.
13. Sun, W.; Ye, B.; Chen, S.; Zeng, L.; Lu, H.; Wan, Y.; et al. Bone Res. 2023, 11 (1), 65. https://doi.org/10.1038/s41413-023-00302-8.
14. Li, S.; Man, Z.; Zuo, K.; Zhang, L.; Zhang, T.; Xiao, G.; et al. Bioact. Mater. 2025, 51, 333–382. https://doi.org/10.1016/j.bioactmat.2025.05.004.
15. Ghasempour, A.; Dehghan, H.; Mahmoudi, M.; Lavi Arab, F. Stem Cell Res. Ther. 2024, 15 (1), 406. https://doi.org/10.1186/s13287-024-04012-8.
16. Stamnitz, S.; Klimczak, A. Cells 2021, 10 (8), 1925. https://doi.org/10.3390/cells10081925.
17. Abdelaziz, A. G.; Nageh, H.; Abdo, S. M.; Abdalla, M. S.; Amer, A. A.; Abdal-Hay, A.; et al. Bioengineering 2023, 10 (2), 204. https://doi.org/10.3390/bioengineering10020204.
18. Wells, C. M.; Harris, M.; Choi, L.; Murali, V. P.; Guerra, F. D.; Jennings, J. A. J. Funct. Biomater. 2019, 10 (3), 34. https://doi.org/10.3390/jfb10030034.
19. Kumari, S.; Katiyar, S.; Darshna; Anand, A.; Singh, D.; Singh, B. N.; et al. Front. Chem. 2022, 10, 1051678. https://doi.org/10.3389/fchem.2022.1051678.
20. Jiang, S.; Wang, M.; He, J. Bioeng. Transl. Med. 2020, 6 (2), e10206. https://doi.org/10.1002/btm2.10206.
21. Piszko, P. J.; Piszko, A.; Kiryk, S.; Kiryk, J.; Horodniczy, T.; Struzik, N.; et al. Biomimetics 2024, 9 (8), 503. https://doi.org/10.3390/biomimetics9080503.
22. Bajer, D.; Kaczmarek, H. Materials 2022, 15 (10), 3667. https://doi.org/10.3390/ma15103667.
23. Lewandowski, R. B. Pol. J. Microbiol. 2025, 74 (2), 232–243. https://doi.org/10.33073/pjm-2025-019.
24. Levengood, S. L.; Zhang, M. J. Mater. Chem. B 2014, 2 (21), 3161–3184. https://doi.org/10.1039/C4TB00027G.
25. Alven, S.; Aderibigbe, B. A. Pharmaceutics 2024, 16 (3), 327. https://doi.org/10.3390/pharmaceutics16030327.
26. Dinesh, H.; Sandhya, S,; Saranya, K,; Ramya, R,; Suganya, P. S,; Pratibha, R.; Pharm. Nanotechnol. 2024, 12 (2), 165–70. https://doi.org/10.2174/2211738511666230607113610
27. Uddandrao, V. V. S.; Eraniappan, S.; Balakrishnan Ramajayam, A.; Singaravel, S.; Roy, A.; Parim, B. N.; Sasikumar, V. Biol. Reprod. Med. 2024, 70(1), 20–37.
28. Elakkiya, K., P.; Bargavi,; S. Balakumar. J Mech Behav Biomed Mater, 2023. 147 (106106): 106106. https://doi.org/10.1016/j.jmbbm.2023.106106
29. Kannan, S,; Bargavi, P,; Kalaiyarasan, M,; Mohammad, R. K, Chitra, S,; Satheesh, K. B,; Sudhisha, Vasudeva, and Asiful H. Seikh. Sustain Chem Pharm 2024, 37 (101438): 101438. https://doi.org/10.1016/j.scp.2024.101438